GPS Nieuwsbrief, **(15)**, 2., Nov. 2000.

Cross-Validation of tropospheric delay variability observed by GPS and SAR interferometry

André van der Hoeven, Ramon Hanssen, Boudewijn Ambrosius

Delft Institute for Earth-Oriented Space Research, Delft University of Technology, Delft, The Netherlands

Abstract. Spatially localized refractivity variations, mainly due to water vapor, are a major source of error in high-precision positioning techniques such as GPS and SAR interferometry. Refractivity induced delay variations can be misinterpreted as, e.g., crustal deformation signal or positioning biases. In this study, signal delay estimates based on SAR observations and simultaneous GPS time series are quantitatively compared. Wind speed and wind direction estimates are used to relate the temporal zenith delays derived from GPS with the spatial slant delays observed by SAR interferometry, assuming a static refractivity distribution transported by the wind. Five case studies show significant correlation between both techniques, mainly limited by the GPS epoch length, zenith averaging, and the degree of similarity in wind direction during the two SAR acquisitions. RMS differences varied between 2 and 9 mm, while the total delay variability spanned 15–60 mm. The results show that it can be possible, under suitable atmospheric circumstances, to approximate the amount of delay variation with wavelengths > 5 km in a strip of a SAR interferogram using GPS, wind speed, and wind direction measurements.

1. Introduction

Atmospheric delay in radio signal propagation is known to be a major source of error in high precision positioning applications such GPS and InSAR (Synthetic Aperture Radar interferometry) [*Bevis et al.*, 1992; *Goldstein*, 1995]. In GPS processing, the dispersive ionospheric part of the delay is largely eliminated by using a linear combination of the two GPS frequencies. The non-dispersive delay in the neutral part of the atmosphere cannot be eliminated this way, and is often estimated as an extra unknown in the GPS data processing [*Brunner and Welsch*, 1993]. In this procedure it is often assumed that there are no horizontal variations and that the observations can be related to zenith delay using a mapping function [*Niell*, 1996]. If the tropospheric delay is the main parameter of interest, it is often decomposed in a hydrostatic ('dry') component, which can be estimated with a 1 mm accuracy using additional pressure measurements, and a 'wet' component which is highly variable, both spatially as well as temporally [*Davis et al.*, 1985]. Nowadays, the wet delay can be derived from the GPS observations at a fixed station with an accuracy of about 6–10 mm in the zenith direction [*Bevis et al.*, 1992; *van der Hoeven et al.*, 1998].

Recently it has been shown that interferometric SAR is able to measure the distribution of the wet delay at the time of the acquisitions with high resolution, provided that local topography is known and no surface deformation occurred [*Hanssen et al.*, 1999]. Often, however, topography or surface deformation are the parameters of interest, and additional wet delay is considered a source of error which can significantly deteriorate the results [*Tarayre and Massonnet*, 1996; *Zebker et al.*, 1997]. As it is not possible to measure the wet delay variation with sufficient accuracy and resolution using standard meteorological techniques, simultaneous GPS observations might aid in the interpretation of the interferometric results. In order to test this hypothesis, a cross-validation between both techniques is performed

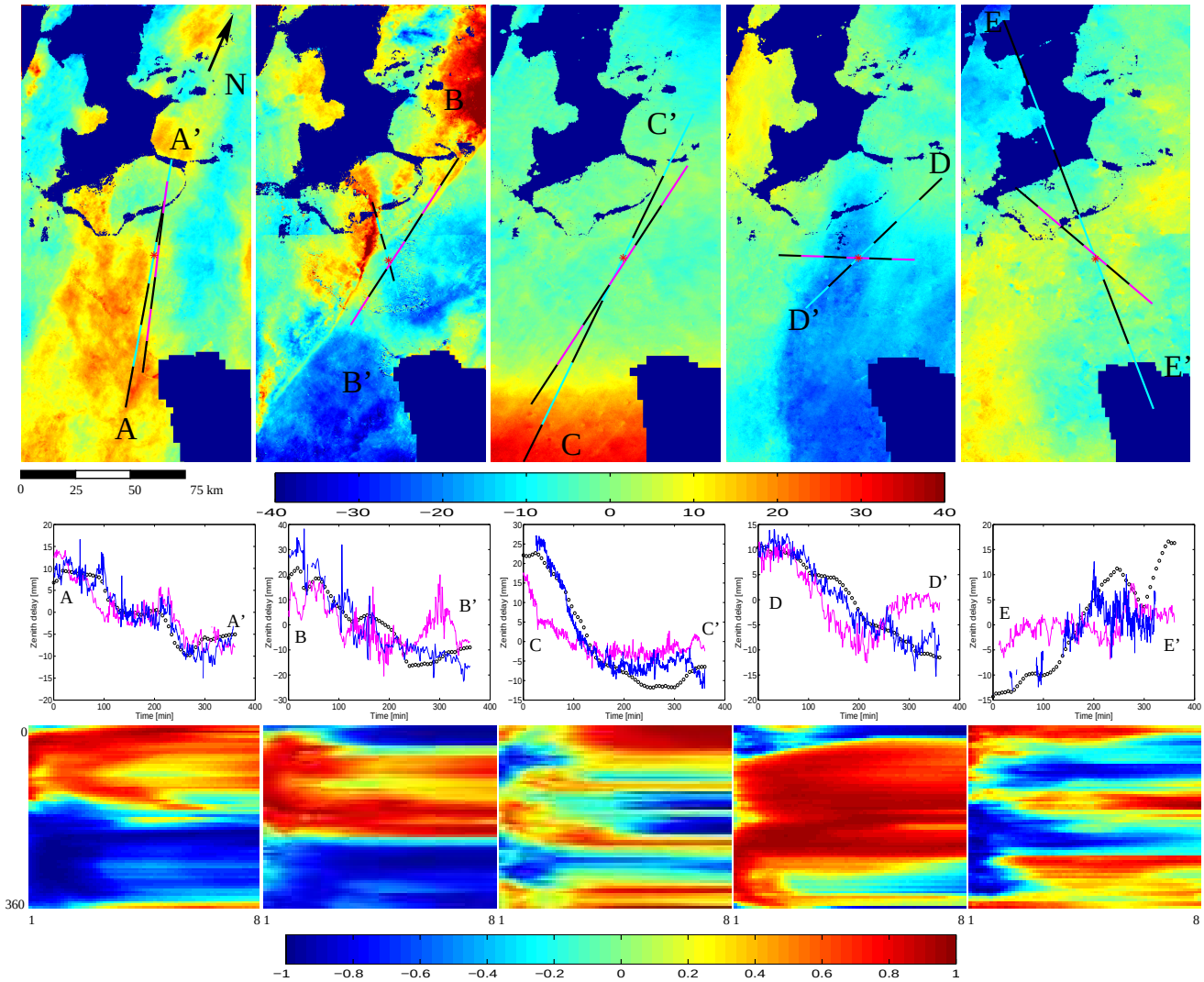

Figure 1. The top row of figures shows the differential SAR interferograms together with the synoptical (black-red) and best-fit profiles (black-yellow) based on GPS delay time series. The blocks in the lines indicate 1-hour time intervals. The red star indicates the position of the GPS station KOSG. The second row of figures shows the GPS time series (red) together with the synoptical profile (blue) and best-fit profile (green). In the last row of figures the correlations are shown between GPS and InSAR for all combinations of wind speed and direction between 1–8 m/s, respectively 0–360°.

in the Netherlands.

2. Observations

Five case-studies are performed, using ERS-1 and ERS-2 SAR data acquired with a one-day interval, hereby excluding crustal deformation signal. Swaths of 200 × 100 km are processed differentially, removing the topographic signal using a reference elevation model [*TDN/MD*, 1997]. For an overview of interferometric processing techniques, see *Massonnet and Feigl* [1998], or *Bamler and Hartl* [1998]. After applying a simple cosine mapping function, the residual signal consists of zenith delay variations in each pair of data acquisitions [*Hanssen et al.*, 1999]. GPS data are obtained at the Kootwijk Observatory for Satellite Geodesy (KOSG), a permanent GPS receiving station. The GPS observations are processed using GIPSY-OASIS while solving for a free network. Data from 13 widely spread IGS stations are used to solve for a number of parameters including satellite clocks, station positions, gradients, and tropospheric delays. The receiver clocks were estimated as white noise processes, while the wet tropospheric delays were estimated as random-walk processes, using the Niell mapping function to convert slant delays from a minimum elevation of 10° to zenith delays [*Niell*, 1996]. The a priori hydrostatic delay is calculated using the Saastamoinen model. To reduce the noise in the zenith delay estimates, the data obtained at a sampling rate of 30 s are averaged into 6 min intervals. The fluctuations in the zenith delays consist of the combined hydrostatic and wet delay—the same contributions as measured by InSAR.

A single GPS station has been selected to investigate the situation when no dense network of GPS receivers is available for the observation period. Unfortunately, this is common practice for most of the situations where research with SAR images is involved. Moreover, although a dense (permanent) network of GPS receivers would enable a direct comparison of the spatial delay variability, there are considerable differences as well. Limitations in this approach are (i) the weighted averaging to zenith delays and (ii) the introduction of interpolation errors due to the inhomogeneous distribution of GPS receivers. If such techniques are applied 'blindly' and used for extracting an atmospheric phase screen from the SAR interferograms, the geophysical interpretation of the results may be more ambiguous than without such a correction.

This study is not an attempt to correct the interferograms, but rather to obtain reasonable estimates of the delay variations and spatial scales to be expected. Such quantitative estimates could significantly improve the interpretation of interferometric SAR data, using only a single GPS receiver as additional source of information.

3. Methodology of comparison

The absolute zenith tropospheric delays derived from GPS constitute time-series at a fixed position. In contrary, InSAR generates a spatial image of the relative zenith delays, differenced between two fixed acquisition times. A conversion needs to be performed to connect the relative-spatial and absolute-temporal observations in order to validate the two data sets.

Two assumptions have been applied to match the two techniques. First, the local atmosphere is treated as a *frozen* atmosphere moving over the area, without changing during a preset time interval [*Taylor*, 1938; *Treuhaft and Lanyi*, 1987]. This refractivity distribution is displaced by the mean wind speed and direction, obtained from surface or radiosonde observations. Second, wind speed and wind direction are assumed to be approximately equal during both observation days. The latter assumption will certainly fail for longer time intervals, but can be more likely for a one-day interval, a common choice for, e.g., DEM generation with InSAR.

Applying these assumptions the GPS time-series can be converted to spatial zenith delay profiles, corresponding with a ground trace in the wind direction and stretched by the wind velocity. These profiles are computed for the two SAR observations from about 4 hours before until about 2 hours after the SAR acquisition (21.41 UTC). The non-symmetric epoch was chosen to avoid delay errors caused by discontinuities in the GPS satellite orbit estimation at the day break, a common problem in contemporary GPS processing. Subsequently the two profiles are differenced, resulting in a differential delay profile, which is comparable to a cross-section in the interferogram. The arbitrary bias between the two sources of data is removed by subtracting their means. This approach is referred to as the *synoptic* approach.

To verify the feasibility of using synoptic wind observations, an alternative approach is performed by rotating and stretching the ground trace over the InSAR-image while recording the correlation between the two profiles. The GPS observations made at the time of the SAR observations are used as axis of rotation. Maximum correlation corresponds with the best-fit between GPS and InSAR. The length of the best-fit ground

trace divided by the total GPS observation time is a measure for the wind speed. The angle of rotation of the best-fit ground trace gives the wind direction relative to the local north. The derived wind speed and direction can then be compared with the synoptic observations for validation.

4. Results

The results of the tropospheric delays estimated by GPS and InSAR are shown in Fig. 1 and Table 1. The first row of Fig. 1 shows the five differential interferograms together with the estimated *best-fit* profile in black-yellow, and the profile based on the *synoptic* observations in black-red. The color changes in the profiles represent 1 hour time intervals. The location of the GPS receiver is indicated by the red star. All interferograms have been converted to relative zenith delay differences, expressed in mm. One colorbar is used, which enables a comparison of the magnitude in variation in every case.

The profiles below the interferograms correspond with the GPS observations (circles), the scaled SAR profile which shows a best fit with the GPS time series (blue), and the SAR profile which is obtained using the surface wind speed and direction (red). In the lower row of plots, correlation coefficients are depicted which resulted in the best fit profile. The vertical axis corresponds with the direction of the profile, the horizontal axis scales the profile with the wind speed in m/s.

Synoptic data from a meteo-station 30 km north of KOSG were used. Average windspeeds were calculated using the data from 21.00 and 22.00 UTC for both days. When the average windspeed was below 2.5 m/s it was assumed that no significant delay changes were present and so this synoptic data was not used in the averaging.

Table 1 lists, for every interferogram, the correlation coefficient between the profiles and the interferometric data. Based on the amount of rotation and stretching of the GPS profile, wind speed and wind direction can be derived. This can be compared with the observed synoptic wind speeds. The comparison between GPS and SAR yields an RMS of difference, which can be compared to the total range of delay variation.

5. Discussion

The five analyzed interferograms represent different combinations of weather, ranging from large scale humidity variation, a narrow and a wide cold front, to a relatively undisturbed, well-mixed boundary layer. Nevertheless, relatively good correlations are found between the GPS and the SAR data. Table 1 shows that the best-fit correlations between GPS and InSAR for the five analyzed interferograms are 0.8 or better, while the estimated wind directions are accurate to within 30° and wind speeds differ maximally 4.0 m/s. In case the synoptic data are used to situate the SAR profile, correlations are 0.75 or better, except for the May 1996 interferogram, where a correlation of −0.01 is found.

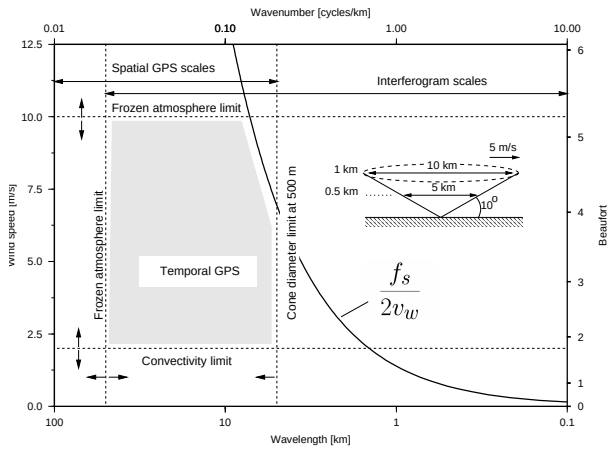

Figure 2. Conceptual sketch indicating the sensitivity ranges of GPS and InSAR delay observations. The shaded region indicates the wavelengths of atmospheric signal which can be detected by GPS time series, under the assumptions presented here. Wavelengths to be detected by a spatial GPS network and by SAR interferometry are indicated by the arrows.

RMS values between GPS and the synoptic SAR profiles are generally worse than those between GPS and the best-fit SAR profiles, which is also indicated by the correlation values. This can be due to (i) a difference in wind speed and direction between the two days, and (ii) the difference in wind speed and direction at surface level and aloft. Furthermore, the assumption of a frozen atmosphere might not be valid in all cases or limited in time.

The sensitivity of GPS observations and SAR interferograms for horizontal refractivity variations at different scales is dependent on the spatial sampling characteristics, the data processing strategy, and the measurement accuracy. Using the frozen atmosphere model with constant wind speed and direction, GPS time series can be regarded as spatial observations along a

Date	Correlation		v_w [m/s]		θ_w [deg]		RMS [mm]		Total range [mm]		
	b.f.	syn	b.f.	obs.	b.f.	obs.	b.f.	syn	SAR_{syn}	$SAR_{b.f.}$	GPS
29-30/8/95	0.95	0.84	5.2	4.1	353	350	2.2	3.5	24	31	19
3-4/10/95	0.90	0.56	2.1	4.1	148	195	6.6	10.3	40	59	35
26-27/03/96	0.95	0.81	8.0	6.2	003	015	3.9	9.1	24	39	31
30/04-01/05/96	0.95	0.57	3.8	3.1	208	075	2.3	6.6	24	29	21
4-5/06/96	0.81	0.44	8.0	3.6	143	115	6.4	8.8	15	20	30

Table 1. Results of the comparison between the GPS time series and two profiles of the SAR interferogram, (i) based on synoptic (syn) wind observations and (ii) based on a best-fit (b.f.) analysis. The observed synoptic wind speed, v_w, and wind direction, θ_w, are listed for comparison. RMS values between the interpolated GPS measurements and the two SAR profiles, and the total range of atmospheric delay variation are shown to compare signal and noise magnitudes.

straight line, with a sampling rate determined by the wind speed. Figure 2 is a conceptual sketch of the sensitivity of GPS and InSAR for atmospheric variation at different wavelengths.

For InSAR, the sensitivity ranges vary theoretically from the resolution cell size to the size of the interferogram. Since measurement noise affects the phase measurements at single resolution cells considerably, an averaging to 100–200 m is used to suppress this noise. For large wavelengths, orbit inaccuracies may cause nearly linear trends in the interferogram. Both effects limit the effective part of the spectrum to wavelengths between 50 km and 100 m.

A GPS network approach is independent of wind speed, assuming the zenith delays can be obtained instantaneous. Effectively, the lower part of the spectrum is not limited, as it is dependent of the amount of receivers and the spatial extend of the network. If the system would be able to measure true zenith delays, the short wavelength part of the spectrum would simply be determined by the spacing between the receivers. Unfortunately, accurate zenith delay estimates are currently only obtained using a spatial and temporal averaging procedure over many satellites above an a priori defined elevation cut-off angle, see the inset at Fig. 2. This procedure effectively acts as a low-pass filter on the spatial wavelengths, with a cut-off wavenumber determined by the minimum elevation angle and the scale height of the wet troposphere, below which most of the horizontal refractivity variations occur. This scale is indicated in the figure as the cone diameter limit.

The use of GPS time series, as described above, implies a dependency of the wind speed. The horizontal lines indicate situations in which the wind speed is either too low or too high for the assumption of a frozen atmosphere to be valid. The left-most vertical line shows that for large spatial scales it will take very long for the atmosphere to drift over the GPS receiver—too long to regard it as *frozen*. The conversion from temporal GPS observations with an effective sampling frequency of $f_s = 1/360$ Hz to a spatial sampling, as a function of wind speed v_w, yields a spatial Nyquist wavenumber of

$$f_N = \frac{f_s}{2v_w}, \tag{1}$$

indicated by the curved line in Fig. 2. It is shown that for wind speeds higher than approx. 7 m/s, the data are undersampled, which might result in aliasing effects. On the other hand, for lower wind speeds the data are effectively oversampled and can be regarded as bandlimited. Low pass filtering should be applied to suppress short wavelengths higher than the bandwidth determined by the cone diameter. The effective range of wavelengths and wind speeds for which GPS time series can be applied is indicated by the shaded region in Fig. 2.

6. Conclusions

When comparing water vapor time-series from a single GPS station with water vapor profiles derived from SAR interferograms it is necessary to have comparable wind speeds and wind directions on both observation days. For the mentioned cases, where the wind speed doesn't differ more than 30 degrees between both days, and the wind speed is equal within 10%, correlations are found in the range of 0.91-0.98. During the situations with larger differences, 30 degrees and 50% respectively, the correlations decreased to 0.81-0.85. This technique only works for a limited strip of the interferogram, i.e., the area where the measured time series covers the SAR image. Nevertheless, the study shows a clear and strong

correspondence between wet signal delay as observed by GPS and InSAR. As such, it aids the interpretation of GPS studies, recognizing the spatial variability of the wet delay and the validity of assumptions on homogeneous or gradient atmospheric models. Currently, the GPS data are used in experiments to parametrize a stochastic model of atmospheric signal for SAR interferometry.

Acknowledgments. The ERS SAR data were kindly provided by ESA. The meteorological data were made available by the Royal Netherlands Meteorological Institute (KNMI).

References

Bamler, R., and P. Hartl, Synthetic aperture radar interferometry, *Inverse Problems*, *14*, R1–R54, 1998.

Bevis, M., S. Businger, T. A. Herring, C. Rocken, R. A. Anthes, and R. H. Ware, GPS meteorology: Remote sensing of atmospheric water vapor using the Global Positioning System, *Journal of Geophysical Research*, *97*, 15,787–15,801, 1992.

Brunner, F. K., and W. M. Welsch, Effect of the troposphere on GPS measurements, *GPS World*, pp. 42–51, 1993.

Davis, J. L., T. A. Herring, I. I. Shapiro, A. E. E. Rogers, and G. Elgered, Geodesy by radio interferometry: Effects of atmospheric modelling errors on estimates of baseline length, *Radio Science*, *20*, 1593–1607, 1985.

Goldstein, R., Atmospheric limitations to repeat-track radar interferometry, *Geophysical Research Letters*, *22*, 2517–2520, 1995.

Hanssen, R. F., T. M. Weckwerth, H. A. Zebker, and R. Klees, High-resolution water vapor mapping from interferometric radar measurements, *Science*, *283*, 1295–1297, 1999.

Massonnet, D., and K. L. Feigl, Radar interferometry and its application to changes in the earth's surface, *Reviews of Geophysics*, *36*, 441–500, 1998.

Niell, A. E., Global mapping functions for the atmosphere delay at radio wavelengths, *Journal of Geophysical Research*, *101*, 3227–3246, 1996.

Tarayre, H., and D. Massonnet, Atmospheric propagation heterogeneities revealed by ERS-1 interferometry, *Geophysical Research Letters*, *23*, 989–992, 1996.

Taylor, G. I., The spectrum of turbulence, *Proceedings of the Royal Society London, Series A*, *CLXIV*, 476–490, 1938.

TDN/MD, TopHoogteMD digital elevation model, Topografische Dienst Nederland and Meetkundige Dienst Rijkswaterstaat, 1997.

Treuhaft, R. N., and G. E. Lanyi, The effect of the dynamic wet troposphere on radio interferometric measurements, *Radio Science*, *22*, 251–265, 1987.

van der Hoeven, A. G. A., B. A. C. Ambrosius, H. van der Marel, H. Derks, H. Klein Baltink, A. van Lammeren, and A. J. M. Kösters, Analysis and comparison of integrated water vapor estimation from GPS, in *Proc. 11th Intern. Techn. Meeting Sat. Div. Instit. of Navig ation*, pp. 749–755, 1998.

Zebker, H. A., P. A. Rosen, and S. Hensley, Atmospheric effects in interferometric synthetic aperture radar surface deformation and topographic maps, *Journal of Geophysical Research*, *102*, 7547–7563, 1997.

A. van der Hoeven, R. Hanssen, and B. Ambrosius. (e-mail: a.g.a.vanderhoeven@lr.tudelft.nl; r.f.hanssen@geo.tudelft.nl; b.a.c.ambrosius@lr.tudelft.nl)